Turkish Journal of Earth Sciences (Turkish J. Earth Sci.), Vol. 21, 2012, pp. 407–414.
doi:10.3906/yer-0908-24 First published online 15 January 2011

A New Late Holocene Eolianite Record from Altınkum Beach, North Cyprus

AHMET EVREN ERGİNAL[1,2], NAFİYE GÜNEÇ KIYAK[3] & TOPÇU AHMET ERTEK[4]

[1] Çanakkale Onsekiz Mart University, Department of Geography, TR–17100 Çanakkale, Turkey
[2] Present address: Ardahan University, Faculty of Humanities and Letters, Department of Geography, TR–75000 Ardahan, Turkey (E-mail: aerginal@gmail.com)
[3] Işık University, Department of Physics, TR–34980 İstanbul, Turkey
[4] İstanbul University, Department of Geography, TR–34459 İstanbul, Turkey

Received 04 September 2009; revised typescripts received 25 May 2010, 24 September 2011 & 03 November 2010; accepted 15 January 2011

Abstract: In this study, we investigated the main depositional characteristics and obtained Optically Stimulated Luminescence (OSL) ages of coastal eolianite on the north coast of Cyprus, where this occurrence had not previously been recorded. Based on EDX/SEM and XRD data and field observations, the studied eolianite that crops out between elevations of 1 m and 14 m a.s.l. is made up predominantly of quartz grains, most of which consist of medium- to fine-grained sand. The rock comprises aragonite, calcite and quartz with lesser amounts of bornite and hematite as accessory minerals. OSL ages indicated that the initial deposition of eolianite sands took place at 1.51±0.21 ka years ago.

Key Words: eolianite, cross-bedding, Holocene, Optically Stimulated Luminescence, North Cyprus

Altınkum Kumsalında (Kuzey Kıbrıs) Yeni Bir Geç Holosen Eolinit Bulgusu

Özet: Bu çalışmada, daha önce bu konuda bir bulgunun kaydedilmediği Kuzey Kıbrıs kıyılarında tespit edilen kıyı eolinitinin başlıca birikim özellikleri ve Işık Uyarımlı Lüminesans yaş verileri araştırıldı. EDX/SEM ve XRD verileri ve arazi gözlemlerine göre deniz seviyesinden itibaren 1–14 m yükseltiler arasında yüzeyleyen eolinitte orta-ince kum boyutundaki kuvars taneleri egemendir. Kayaç aragonit, kalsit ve kuvars dışında az oranda bornit ve hematit içerir. OSL yaşları Eolinit kumlarının ilk birikim yaşının günümüzden 1.51±0.21 bin yıl önce biriktiğini göstermektedir.

Anahtar Sözcükler: eolinit, çapraz tabakalaşma, Holosen, Işık Uyarımlı Lüminesan, Kuzey Kıbrıs

Introduction

As carbonate-cemented fossil dune deposits of mostly Quaternary age (see Fairbridge & Johnson 1978 and Brooke 2001 for detailed review), eolianites yield key clues in understanding not only Late Quaternary to Holocene sea-level variations but also wind-blown sediment transportation dynamics acting on coastal environments. The distribution, composition, cementation characteristics and deposition age of these indurated rocks throughout the world's coastlines have been discussed recently by Brooke (2001) and Frébourg *et al.* (2008). As their characteristics are similar to those of recent coastal dunes, such as cross-bedding structures, sand-dominated grain size and shore-parallel long axes, these rocks provide records of both past coastal wind-blown sand drift dynamics and of complex interactions between eolian and colluvial-fluvial deposition processes in coastal environments (Fornós *et al.* 2009).

The mineral and grain composition, as well as the cement micro-morphology of eolianites, provide insights into the depositional history of coastal dunes. These rocks have also some diagnostic characteristics, such as high carbonate content, different cementation patterns (Frébourg *et al.* 2008), fossil root casts or rhizoliths (Klappa 1980) and palaeosol (Tsatskin *et al.* 2009). Thus, several authors have stressed the significance of eolianites to ascertain late Quaternary to Holocene coastal morpho-dynamics and sea-level changes (Kelletat 1991; Woodroffe *et al.* 1995; Kiyak & Erginal 2010).

Brooke (2001) showed the global distribution of eolianites in 89 different coastal localities all over the world, of which those located on the Mediterranean coasts occur on the eastern coasts of the Iberian Peninsula and the islands of Mallorca, Corsica, and Sardinia, as well as in Lebanon and Israel. Although the presence of eolianite on the south Cyprus coast was recorded by Poole & Robertson (1991) on the Akrotiri Peninsula, and recently by Butzer & Harris (2007) near Paphos, Episkopi and Zyyi, no eolianite record on the north Cyprus coast has previously been made. Thus, this paper deals, for the first time, with the composition, depositional characteristics and age of eolianite on the coast of the Karpasia (Καρπασία or Karpaz) Peninsula in northeast Cyprus (Figure 1) using energy dispersive x-ray spectroscopy/ scanning electron microscopy (EDX/SEM) and x-ray diffraction (XRD). Six samples of eolianite were dated using optically stimulated luminescence (OSL).

Site Description

The studied eolianite (Figure 1) is located on Altınkum beach at the northeast end of the 55–km long Karpasia Peninsula (latitude 35°38'46'' to 35°38'30'' N, longitude 34°32'40'' to 34°33'26'' E). Geologically, this peninsula is the NE extension of the Kyrenia range in North Cyprus, comprising the Kyrenia (Girne) terrain, which is one of the main geological units on the island of Cyprus (Dreghorn 1978; Poole & Robertson 1991). To the north of the studied beach, the Kyrenia terrain comprises the middle Miocene Kythrea formation, consisting of greywacke, marls, and especially sandstone.

The long-term temperature and precipitation data recorded by the Girne and Lefkoşa meteorology stations show that a typical Mediterranean climate regime prevails in North Cyprus. The average air temperatures and precipitations are 19.9–19.3°C and 481–310 mm, respectively. The average maximum and minimum sea water temperatures range between 28.6°C (August) and 15.8°C (February). The studied eolianite underlies a broad dune field extending approximately 500 m north–south and 1 km east–west that is covered by dune grasses and, to a lesser extent, shrubs.

Methods

Sampling and Microanalyses

A total of six samples from two different sites were extracted for grain size determination and microanalysis. Structural and geomorphological characteristics of the eolianite outcrops were noted during field studies. The element composition and micromorphological features of eolianite samples were examined using a Phillips XL-30S FEG Scanning Electron Microscope equipped with EDX detector. X-ray Diffractometry (Phillips X’Pert Pro) was used to determine the mineral content. The analyses were carried out in the Materials Research Center of the İzmir Institute of High Technology.

Sample Preparation and Measurements for OSL Dating

The six samples were evaluated by the luminescence (optically stimulated luminescence-OSL) dating technique. This technique is based on the radiation dose (equivalent or palaeodose) estimate accumulated in quartz extracted from sediment (Aitken 1998; Murray & Mejdahl 1999). The quartz grains were extracted from sediment using a chemical technique. First the quartz grains measuring 90–180 μm were wet sieved and then treated with HCl to remove carbonates, and with H_2O_2 for the removal of organic material. Then the grains were etched with HF for feldspar separation, and each sample was checked for the absence of feldspar contamination using infrared stimulation.

The OSL signals were measured with an automated Risø TL/OSL reader (model TL/OSL-DA-15) equipped with an internal $^{90}Sr/^{90}Y$ beta source (~0.1 Gy s^{-1}). For the stimulations, blue light emitting diodes (LEDs) (470 nm, ~40 mW cm^{-2}) and IR LEDs (880 nm, ~135 mW cm^{-2}) were used through an EMI 9635QA photomultiplier tube, fitted with Hoya U-340 filters of 7.5 mm total thickness (Bøtter-Jensen 1997). The dose rate required for age calculation was estimated from spectroscopic measurements in-situ using conversion factors presented by Olley *et al*. (1996). The OSL dating was carried out at the Optical Luminescence Laboratory in the Physics Department of Işık University, Turkey.

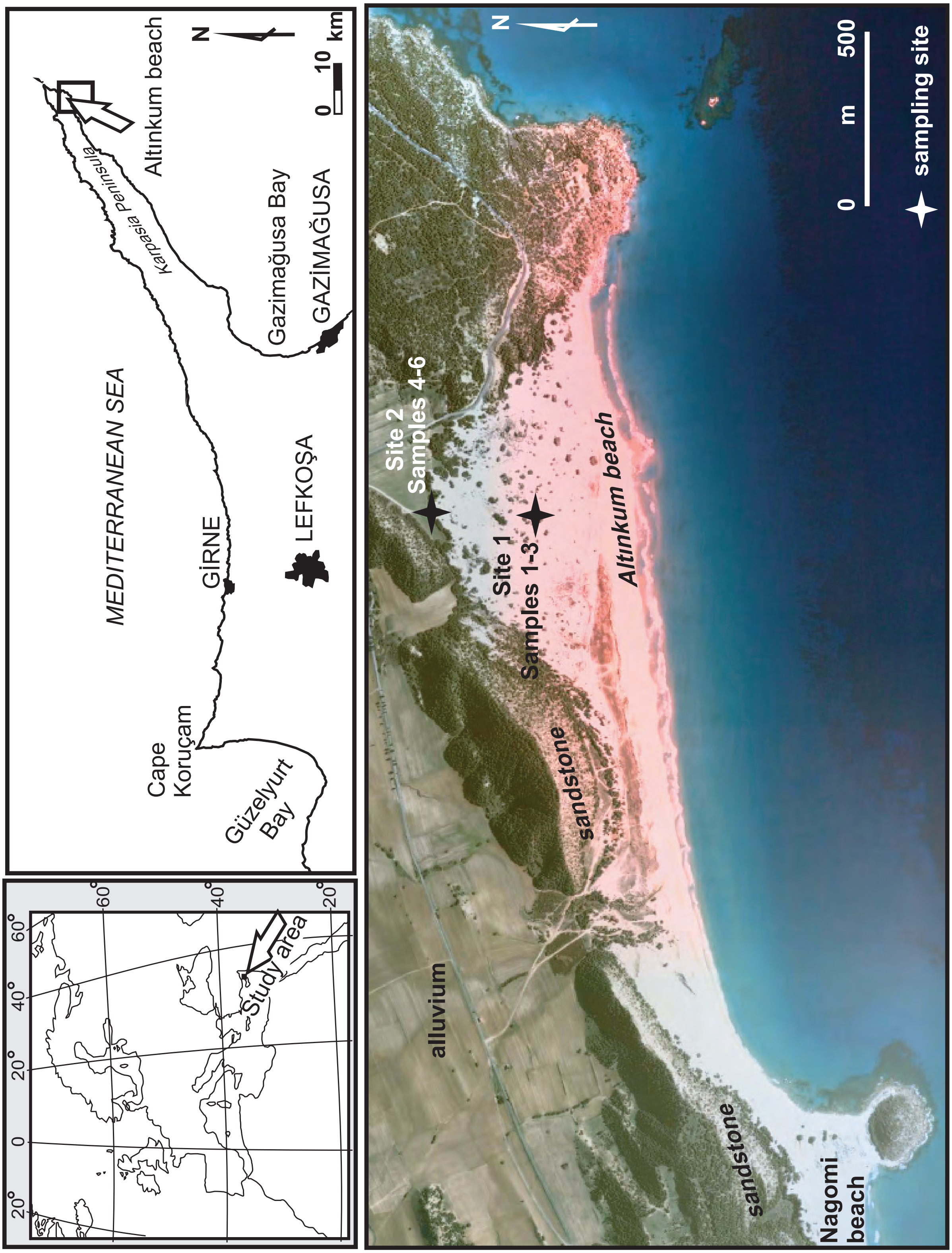

Figure 1. Location map and sampling sites shown on a satellite image (GoogleEarth 2007). Numbers indicate samples.

Equivalent Dose (D_e) and OSL Age Evaluation

The OSL age is obtained from the ratio of equivalent dose (D_e) accumulated in quartz during the burial time of sediment material to environmental dose rate. The single-aliquot regenerative-dose (SAR) protocol is applied to obtain the equivalent dose in quartz, as extensively described in the literature (Mejdahl & Bøtter-Jensen 1994; Murray & Mejdahl 1999; Murray & Wintle 2000). In this technique, the natural OSL signal is compared with the OSL signals produced by known laboratory doses. The natural OSL dose value is interpolated on the growth curve constructed with OSL regenerative dose data to obtain the corresponding laboratory dose.

The dose response curve of corrected OSL signals between 0 and 5 Gy shows a slight exponential behaviour for quartz extracted from a representative sediment sample, ENT01 (Figure 2). The equivalent dose D_e of the sample was obtained from the interpolation of corrected natural signals on the dose-response curve. The first regenerative dose was repeated to view repeatability on the dose-response curve in order to check the reliability of OSL measurements. For the OSL age evaluation, the dose rate of the radiation environment was derived from the gamma dose rates measured in the field and concentrations in the sediment samples of the major radioactive isotopes of the uranium and thorium series, and of potassium (Olley *et al*. 1996). The cosmic ray contribution to total dose rate was evaluated using altitude, latitude and depth from the surface of each sample location (Prescott & Hutton 1988). The equivalent dose, dose rates and OSL ages obtained are presented in Table 1, with the number of aliquots evaluated for each sample.

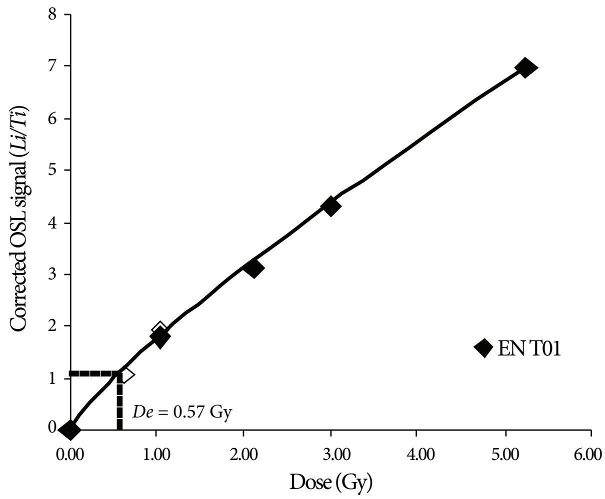

Figure 2. Dose response curve for sample ENT01. Corrected OSL dose values are fitted with a mathematical function between 0 and 5 Gy. First open diamond indicates the natural dose, second open diamond is the repeated dose on the dose response curve.

Results and Discussion

Composition and Structure of Eolianite

The studied eolianite exposures can be observed due to the stripping of dune sands by wind activity and surface wash during heavy rainfalls, giving rise to

Table 1. OSL ages in (ka), SAR dose values of samples in (Gy), and dose rate of radiation environment in (Gy/ka), where n is the number of aliquots evaluated.

Lab code	Longitude (North)	Latitude (East)	Depth (cm)	Age (ka)	SAR De (Gy)	n	Dose rate Gy/ka)
ENT01	4°33´02″	35°38´37″	20	0.41±0.09	0.57±0.12	8	1.38
ENT02	34°33´02″	35°38´37″	100	0.59±0.12	0.79±0.16	7	1.33
ENT03	34°33´02″	35°38´37″	210	0.64±0.05	0.82±0.06	8	1.29
ENT04	34°33´02″	35°38´46″	10	0.81±0.09	1.17±0.13	6	1.44
ENT05	34°33´02″	35°38´46″	200	0.97±0.18	1.26±0.2	8	1.31
ENT06	34°33´02″	35°38´46″	400	1.51±0.21	1.91±0.26	8	1.26

the emergence of mesa-like forms in several places. The eolianite is mostly composed of cross bedded laminae having an average dip strike trend of N40°E, similar to that of the present coastline. Cross beds dip towards the northwest and southeast at angles between 2° and 26°, showing the bidirectional effects of northwesterly and southeasterly winds. The bottom foreset beds are, however, steeper and reach up to 30° (Figure 3a) especially at lower levels close to the present beach.

Petrographically, the eolianite is weakly cemented yellow sandstone in composition, consisting mainly of fine- to medium-size grains as well as abundant (65.5%) $CaCO_3$ based on calcimetric measurements. In some places, numerous angular fragments of pumice were also found to have combined within the dune sands. Confirmed by SEM images, grain size measurements show that grains ranging between 0.5 mm and 0.25 mm are dominant (38.9%), followed by 0.25–0.125 mm (35.62%), suggesting the predominance of medium to fine sand. Coarse and very coarse sands (>0.5 mm) average 15%, while fine materials (<0.163 mm) are found in lesser amounts of 10%. The abundance of medium- to coarse-grained sands with thick (>1 m) sets of cross beds are probably indicative of ascending dunes on steep slopes behind the dune field. In fact, the study area is backed by sandstones of the Kythrea formation, suggesting that eolian sand drift took place in a source-bordering local environmental setting.

Grains are moderately to well rounded and their surfaces are coated by very thin (1–2 μm) carbonate envelopes that are not fresh in appearance (Figure 3b) in proportion to those of active dune sands (Figure 3c). SEM images show that there is an obvious difference between old eolianite sands and present beach sands (Figure 3d, e). Some grains seem to be amalgamated by thin meniscus bridges of calcite cement. EDX analyses of this cement demonstrate the predominance of O (42.91%), Ca (34.58%) and C (17.98%). The rest of the composition consists, in decreasing order, of Si>Fe>Mg>Na>Al>K, having only an average of 4.5%. Based on XRD data, for the bulk eolianite sample, the rock contains, in decreasing proportions, quartz, aragonite, calcite, bornite and hematite, some of which were possibly derived from neighbouring cliffs of Miocene sandstone.

OSL Ages and Significance

The OSL ages showed the existence of two phases of eolian dune sand deposition. Sampling site 1 shown in Figure 1 is located about 100 m from the present shoreline. This fine- to medium-grained sequence is composed of foreset beds of cross-stratified laminae. The weakly cemented first three samples (ENT01, ENT02 and ENT03) collected from this area yielded ages ranging between 0.41±0.09 ka and 0.64±0.05 ka, suggesting a deposition interval of 230 years. The other three samples (ENT04, ENT05 and ENT06), which are relatively harder, were extracted from sampling site 2 located 500 m north of the beach where the eolianite crops out at 14 m above the present sea-level. In terms of facies architecture, this outcrop shows characteristics of cliff-front dune and ascending dune deposits based on the presence of a single larger-scale cross bedding in its stratigraphy (Fornós *et al.* 2009). The OSL results for these samples indicate older ages, suggesting initial deposition of wind-blown sands occurring 1.51±0.21 ka before the present, and that the second generation, being closer to the beach, represents younger eolianite. Consequently, the OSL ages reveal that the Altınkum eolianite forms a new record for late Holocene eolianites. Such young deposition ages have not been documented before on the Mediterranean coast. Some examples were suggested previously by Xitao (1988) and Qihao & Yanji (1990) on the Fujian and Guangdong coasts of southern China.

The two young phases of aeolian deposition, indicated by their OSL ages, provide important insights into the rate at which coastal dunes begin to become lithified under a Mediterranean climate. Both coarse sands and detrital mineral grains confirmed by XRD data suggest derivation from local sources, namely the Miocene Kythrea sandstone of the Kyrenia terrain. Furthermore, the sequence does not include any marine-sourced component to suggest, for instance, wind-blown drift of exposed marine shelf sediments during a low sea-level stage. Previous geo-archaeological studies on Holocene sea-level variations along the Turkish Mediterranean coast revealed that the sea-level has risen during the last 3000 years from a level 2 m lower 4000 years ago (Kayan 1988). For instance, the sea-level on the coast of Israel was suggested to have not been lower

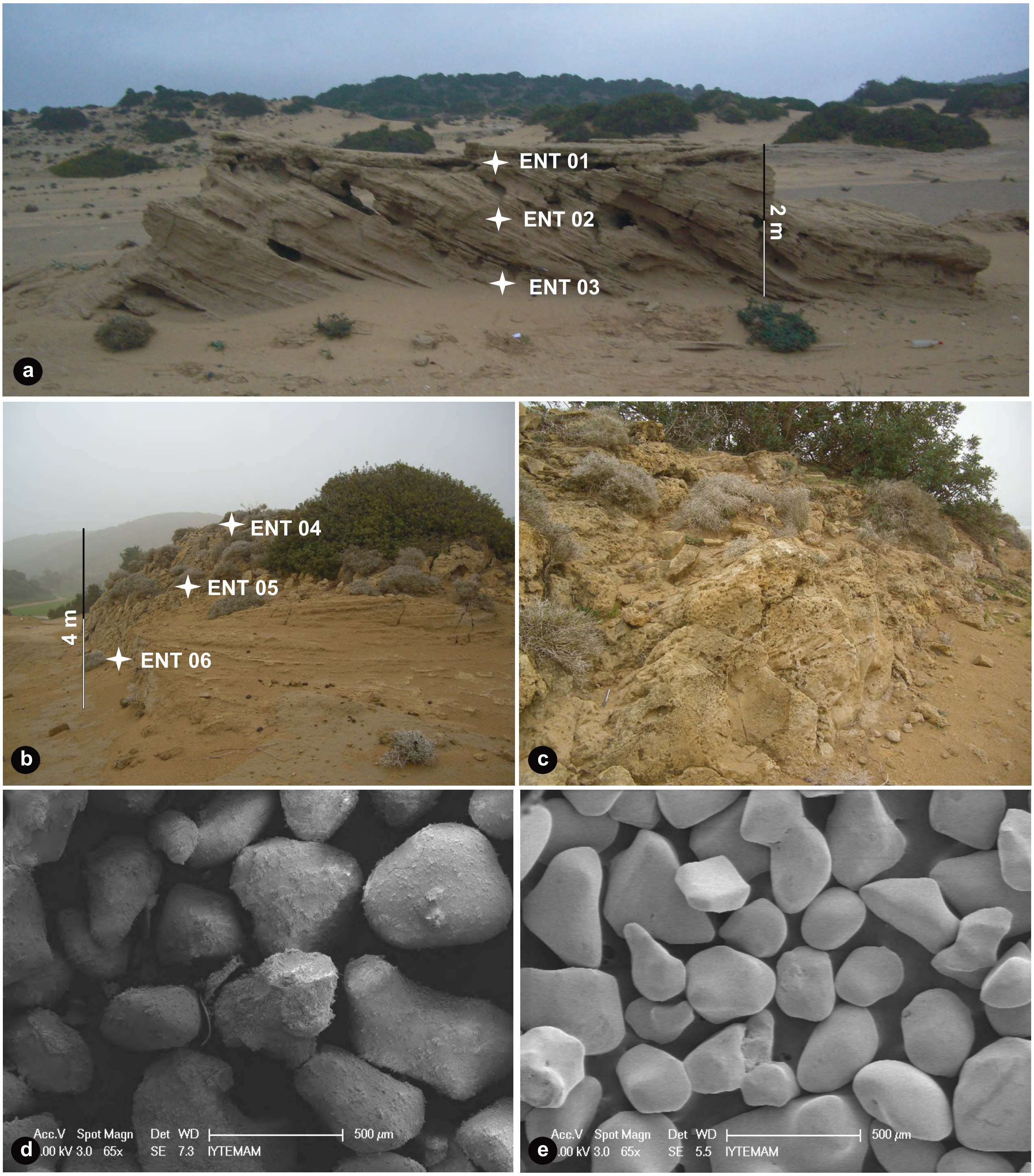

Figure 3. **(a)** Cross-bedding structure of the studied eolianite. **(a)** and **(b, c)** show sampling sites 1 and 2, respectively, in Figure 1. SEM images show clear difference between eolianite sands **(d)** and present beach sands **(e)**.

than –3 m between 3200 and 2000 years before the present, based on archaeological data and numerical model predictions (Sivan *et al*. 2001). In the last 2000 years, Lambeck & Bard (2000) suggested a relative sea-level rise of 0.5 m. During the last 1500 years and the last century, Morhange *et al*. (2001) proposed a near stable sea-level for the southern coast of France. Thus, it can be suggested with reference to existing geo-archaeological data that the Altınkum eolianite was deposited as shoreline dunes when sea level was similar to the present level. The relatively rapid lithification of the aeolian sands appears related to fluctuating sediment moisture levels induced by the semiarid climatic conditions of the island.

Conclusions

The aeolianite in this study is the first recorded from the North Cyprus coast, and is significant for the interpretation of the evolution of both ancient and recent coastal dune dynamics in that area. We recognized the existence of two generations of young aeolianites; namely (1) tighter cemented larger-scale cross-stratified older aeolianite suggestive of cliff-front ascending aeolian deposition, and (2) steeply laminated younger aeolianite deposited 500 m north of the beach as a second stage of aeolian sand drift. OSL dating estimations indicate that the initial development of the coastal dunes took place at 1.51±0.21 ka before the present when the sea-level was close to its present position.

References

Aitken, M.J. 1998. *An Introduction to Optical Dating: The Dating of Quaternary Sediments by the Use of Photon-stimulated Luminescence*. Oxford University Press, Oxford and New York.

Bøtter-Jensen, L. 1997. Luminescence techniques: instrumentation and methods. *Radiation Measurements* **17**, 749–768.

Brooke, B. 2001. The distribution of carbonate eolianite. *Earth-Science Reviews* **55**, 135–164.

Butzer, K.W. & Harris, S.E. 2007. Geoarchaeological approaches to the environmental history of Cyprus: explication and critical evaluation. *Journal of Archaeological Science* **34**, 1932–1952.

Dreghorn, V. 1978. *Landforms in the Girne Range, Northern Cyprus*. MTA Publications, **172**, Ankara.

Fairbridge, R.W. & Johnson, D.L. 1978. Eolianite. *In*: Fairbridge, R.W. & Bourgeois, J. (eds), *The Encyclopedia of Sedimentology*. Dowden, Hutchinson and Ross, Stroudsburg, PA, 279–282.

Fornós, J.J., Clemmensen, L.B., Gómez-Pujol, L. & Murray, A.S. 2009. Late Pleistocene carbonate aeolianites on Mallorca, Western Mediterranean: a luminescence chronology. *Quaternary Science Reviews* **28**, 2697–2709.

Frébourg, G., Hasler, C-E., Le Guern, P. & Davaud, E. 2008. Facies characteristics and diversity in carbonate eolianites. *Facies* **54**, 175–191.

Kayan, I. 1988. Late Holocene sea-level changes on the western Anatolian coast. *Palaeogeography, Palaeoclimatology, Palaeoecology* **68**, 205–218.

Kelletat, D. 1991. Geomorphological aspects of eolianites in Western Australia. *In*: Bruckner, H. & Radtke, U. (eds), *Von der Nordsee bis zum Inischen Ozsean*. Franz Steiner Verlag, Stuttgart, 181–198.

Kiyak, N.G. & Ergİnal, A.E. 2010. Optical Stimulated Luminescence dating study of eolianite on the Island of Bozcaada, Turkey: preliminary results. *Journal of Coastal Research* **26**, 673–680. doi: 10.2112/08-1169.1.

Klappa, C.F. 1980. Rhizoliths in terrestrial carbonates: classification, recognition, genesis, and significance. *Sedimentology* **26**, 613–629.

Lambeck, K. & Bard, E. 2000. Sea-level change along the French Mediterranean coast since the time of the last Glacial Maximum. *Earth and Planetary Science Letters* **175**, 203–222.

Mejdahl, V. & Bøtter-Jensen, L. 1994. Luminescence dating of archaeological materials using a new technique based on single aliquot measurements. *Quaternary Science Reviews (Quaternary Geochronology)* **13**, 551–554.

Morhange, C., Laborel, J. & Hesnard, A. 2001. Changes of relative sea level during the past 5000 years in the ancient harbor of Marseilles, Southern France. *Palaeogeography, Palaeoclimatology, Palaeoecology* 16**6**, 319–329.

Murray, A.S. & Mejdahl, V. 1999. Comparison of regenerative-dose single-aliquot and multiple-aliquot (SARA) protocols using heated quartz from archaeological sites. *Quaternary Science Reviews (Quaternary Geochronology)* **18**, 223–229.

Murray, A.S. & Wintle, A.G. 2000. Luminescence dating of quartz using an improved single-aliquot regenerative-dose protocol. *Radiation Measurements* **32**, 57–73.

Olley J.M., Murray A.S. & Roberts R.G. 1996. The effects of disequilibria in the uranium and thorium decay chains on burial dose rates in fluvial sediments. *Quaternary Geochronology* **15**, 751–760.

Poole, A.J. & Robertson, A.H.F. 1991. Quaternary uplift and sea-level change at an active plate boundary, Cyprus. *Journal of the Geological Society, London* **148**, 909–921.

Prescott, J.R. & Hutton, J.T., 1988. Cosmic ray and gamma ray dosimetry for TL and ESR. *Nuclear Tracks Radiation Measurements* **14**, 223–227.

Qihao, X. & Yanji, F., 1990. Features of geomorphology and sedimentology of dune rocks and dunes at the coast of Guangao, Dongshan, and other areas in Guangdong and Fujian, China. *Tropic Oceanology* **9**, 61–69.

Sivan, D., Wdovinski, S., Lambeck, K., Galili, E. & Raban, A. 2001. Holocene sea-level changes along the Mediterranean coast of Israel, based on archaeological observations and numerical model. *Palaeogeography, Palaeoclimatology, Palaeoecology* **167**, 101–117.

Tsatskin, A., Gendler, T.S., Heller, F., Dekman, I. & Frey, G.L. 2009. Towards understanding paleosols in Southern Levantine eolianites: Integration of micromorphology, environmental magnetism and mineralogy. *Journal of Mountain Science* **6**, 113–124.

Woodroffe, C.D., Murray-Wallace, C.V., Bryant, E.A., Brooke, B.P., Price, D.M. & Heijnis, H. 1995. Late Quaternary sea-level highstands from the Tasman Sea: evidence from Lord Howe Island. *Marine Geology* **125**, 61–72.

Xitao, Z. 1988. Eolianites in Fujian, China. *Journal of Coastal Research Special Issue* **3**, 83–90.